

Decisive or Distracted: the Effects of United States Constraint on Security Networks — Supplementary Materials

Ha Eun Choi^a, Scott de Marchi^b, Max Gallop^c, Shahryar Minhas^d

^a*Department of Political Science, University of Potsdam*

^b*Department of Political Science, Duke University*

^c*Department of Political Science, Strathclyde University*

^d*Department of Political Science, Michigan State University*

Abstract

This document contains supplementary materials for “Decisive or Distracted: the Effects of United States Constraint on Security Networks.” It includes additional details on the construction of the US distraction index, robustness checks with alternative model specifications, results for alignment with Russia, sensitivity analyses with varying dimensionality of the latent factor model, and simulation studies validating our measurement approach.

Keywords: security networks, U.S. foreign policy, latent variable models, network analysis, measurement models

*Alphabetical order signifies equal authorship, all mistakes are our own. Replication data for this article can be found at <https://doi.org/10.7910/DVN/EGLKEI>. Additional replication material and instructions are available at <https://github.com/s7minhas/plutonium>. Shahryar Minhas acknowledges support from the NSF, Award 2017180.

Email addresses: choi@uni-potsdam.edu (Ha Eun Choi), demarchi@duke.edu (Scott de Marchi), gallop@strathclyde.edu (Max Gallop), minhassh@msu.edu (Shahryar Minhas)

Appendix

Contents

A.1Construction of US distraction index	2
A.1.1 Variables used to generate US distraction index	2
A.1.2 Scree plot for US distraction index	3
A.1.3 Factor Loadings	4
A.1.4 Descriptive Statistics	5
A.2Results when measuring alignment against Russia	6
A.3Varying the Dimensionality of the Multiplicative Effect	9
A.4Country Fixed Effects Robustness Check	11
A.5Simulation Study for Latent Factor Measurement	14
A.5.1 Data-Generating Process for Votes	14
A.5.2Assessing Recovery of the True Positions	15

A.1. Construction of US distraction index

In this section, we provide further details on the construction of our US distraction index.

A.1.1. Variables used to generate US distraction index

Here we list out the sources for the variables that we use to generate our US distraction index.

Table A.1: Variables for generation of US Distraction Index

Variables	Source
Defense spending	?, ?
Troop levels, by region	?, ?
US Casualties	?, ?
Market Crises	?
Economic variables	?

A.1.2. Scree plot for US distraction index

Figure A1 illustrates the cumulative proportion of variance accounted for by each of the factors in the top panel, and in the bottom the variance of each factor. A PCA with two latent variables explained over 75% of the variance in the raw data.¹

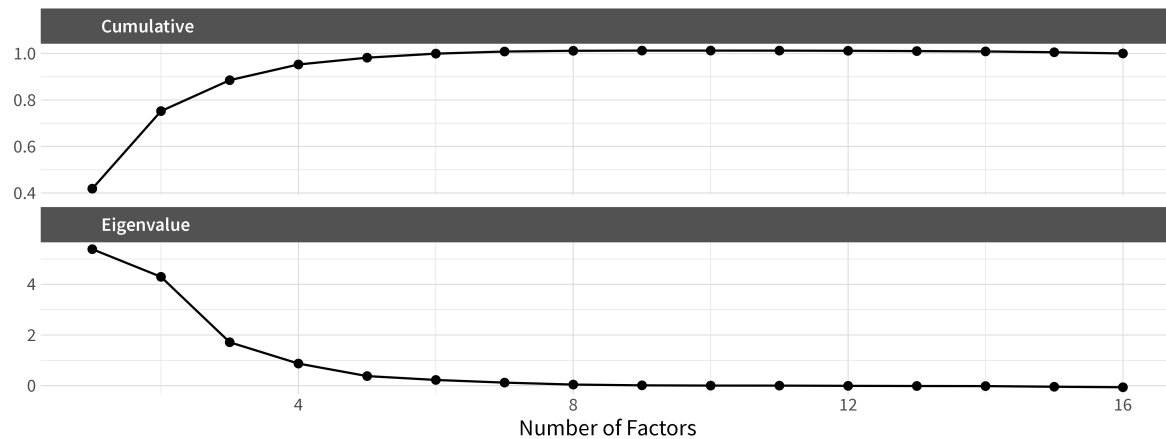


Figure A1: Scree plot of constraint PCA.

¹A possible third factor, which we did not include, has the employment rate as its most salient component. The interpretation of this factor as "economic shocks" is not, however, clear given the other factor loadings and we accordingly leave economic causes of constraint to future work.

A.1.3. Factor Loadings

Figure A2 below shows factor loadings of each component variable for three latent factors, representing active US conflicts (F_1), US defense spending / commitments (F_2), and US economic shocks (F_3).

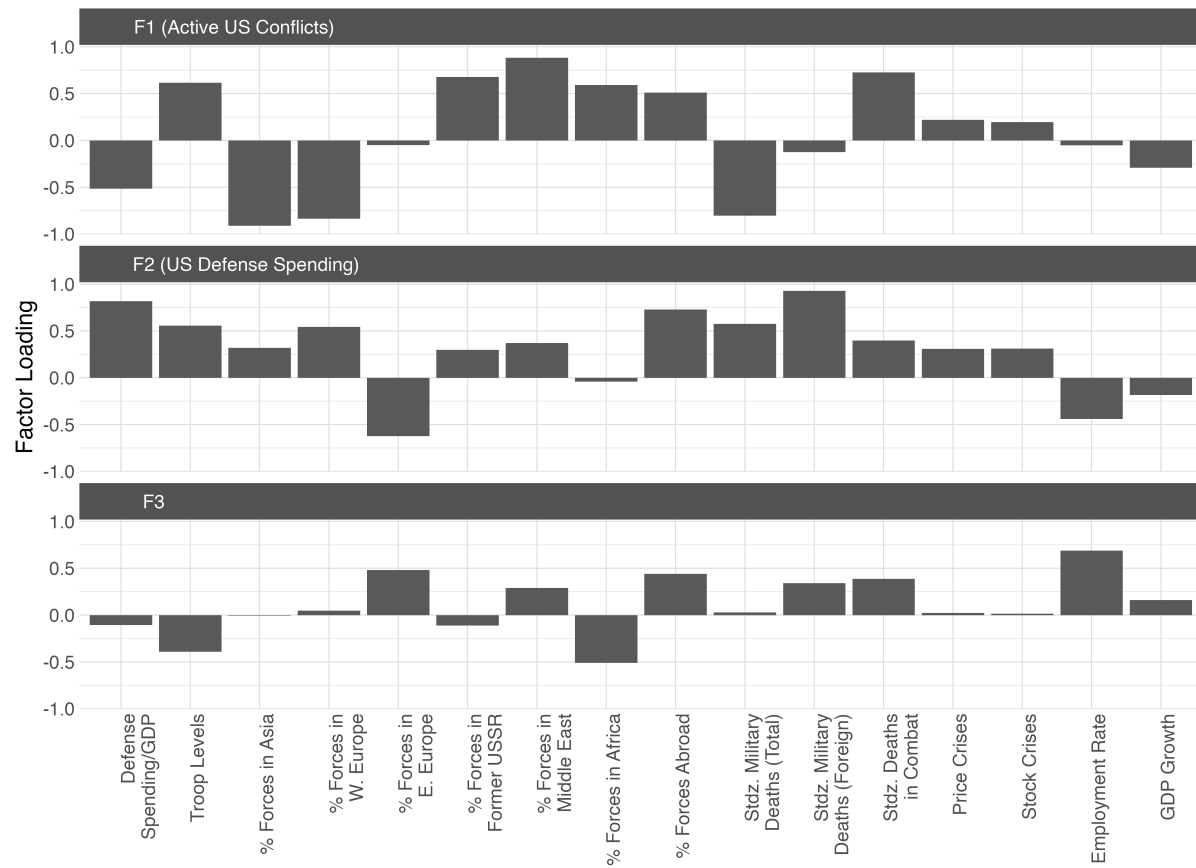


Figure A2: Loadings of constraint PCA

A.1.4. Descriptive Statistics

Here we show descriptive statistics for each of the variables used in our analysis of how countries aligned towards China during times of US distraction.

	Unique (#)	Missing (%)	Mean	SD	Min	Median	Max	
Diplomatic Alignment	2750	5	0.2	0.8	-1.0	0.6	1.0	
Economic Alignment	2888	1	0.0	0.8	-1.0	0.3	1.0	
F1 (Active US Conflicts)	22	0	0.0	1.0	-1.7	0.0	1.4	
F2 (US Defense Spending)	22	0	-0.0	1.0	-1.6	0.1	1.5	
Polity	22	7	-0.0	1.0	-2.3	0.5	1.0	
GDP	2705	7	0.0	1.0	-2.3	-0.1	2.5	
Logged Capital Distance to China	139	0	0.0	1.0	-2.0	-0.2	2.7	

Figure A3: Descriptive Statistics



A.2. Results when measuring alignment against Russia

Here we visualize the results of the model when focusing on how alignment with respect to Russia instead of China. Figure A4 shows the parameter estimates for our diplomatic alignment model with random country effects. Figure A5 shows the parameter estimates for our diplomatic alignment model with varying effects of the distraction measures by polity categories.

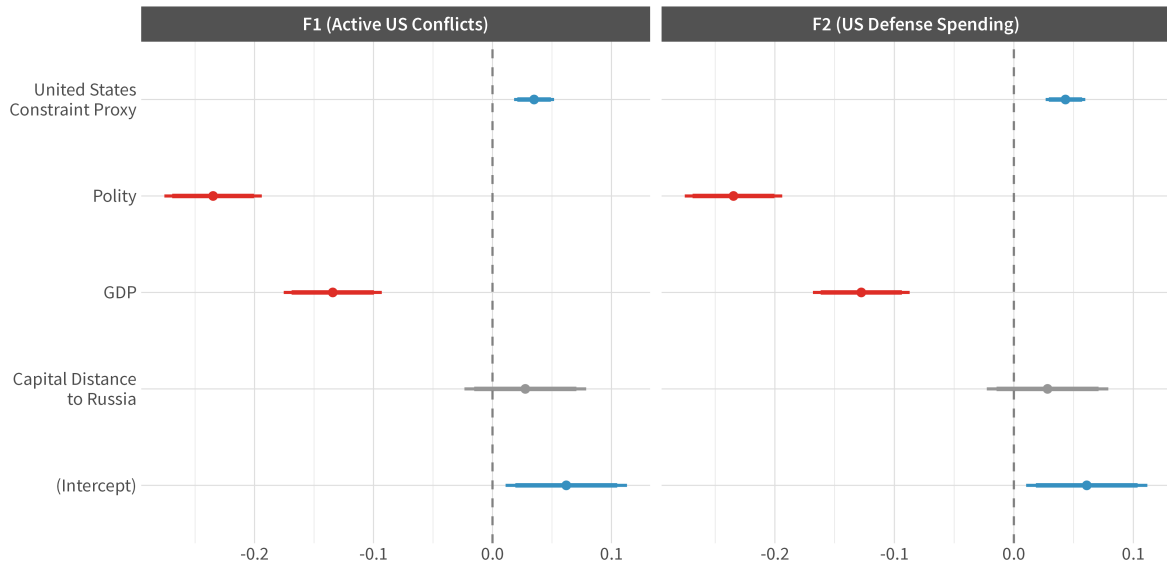


Figure A4: Parameter estimates from hierarchical model on diplomatic similarity with random country effects. Each column shows the results with a different distraction measure that is labeled in the facet on the top of the plots. Points represent average value of parameters, thicker line represents the 90% confidence interval, and thinner the 95%.

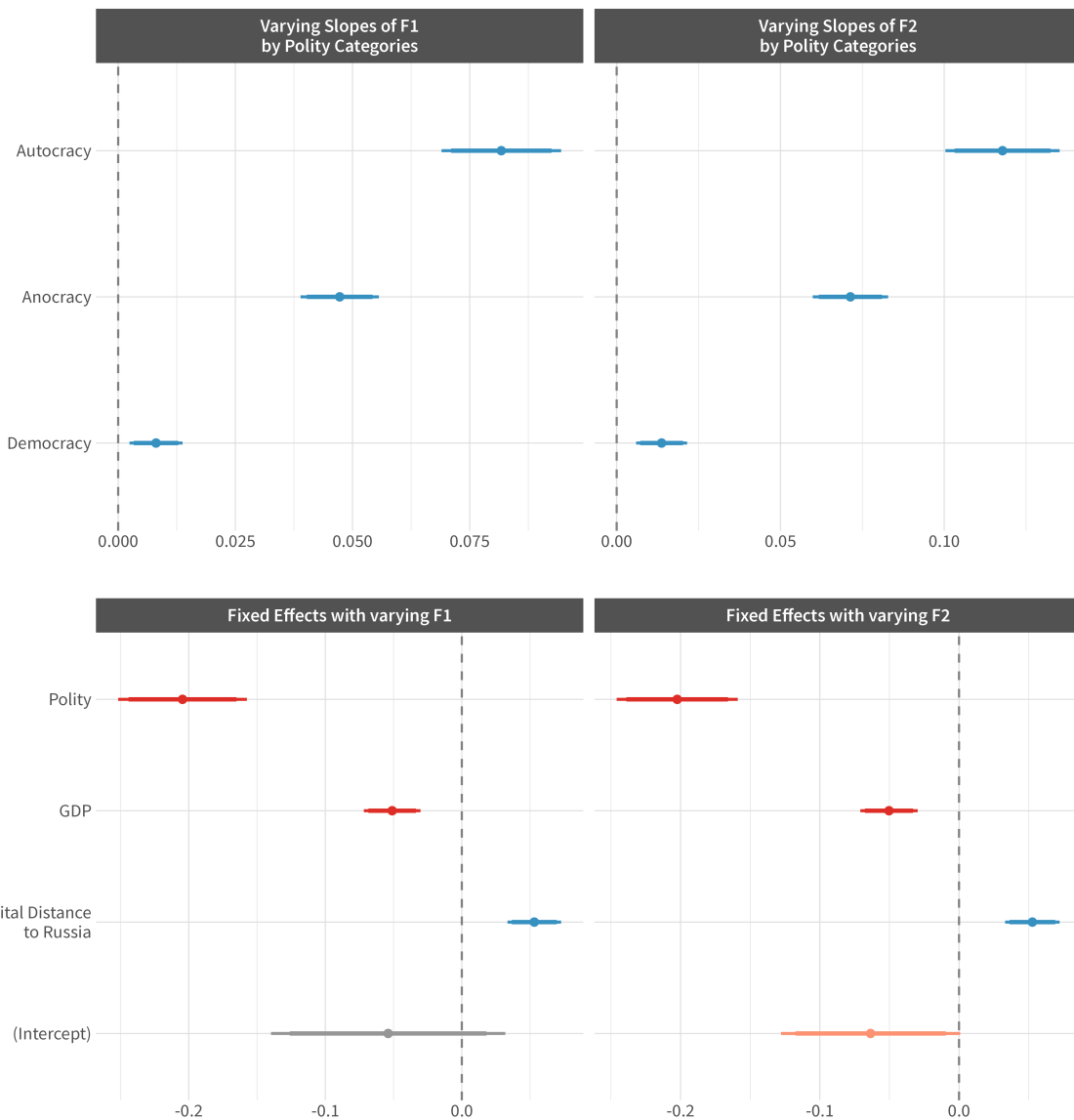


Figure A5: Parameter estimates from hierarchical model on diplomatic similarity with varying effects of the distraction measures by polity categories. Top panel shows how the distraction measures vary by polity categories and bottom the fixed effects, each column again represents the results of one model. Points represent average value of parameters, thicker line represents the 90% confidence interval, and thinner the 95%.

When we estimate a model allowing the effect of distraction to be conditional on political institutions. Across our two measures of distraction, autocracies are most prone to move towards Russia when the US distracted, democracies least prone, and anocracies in the middle.

A.3. Varying the Dimensionality of the Multiplicative Effect

Here we visualize the results of the model with varying degree of the dimension of the multiplicative effects ($K=5$). Figure A6 shows the parameter estimates for our diplomatic alignment model with random country effects. Figure A7 shows the parameter estimates for our diplomatic alignment model with varying effects of the distraction measures by polity categories. Our results are consistent with a 2 dimensional latent factor space.

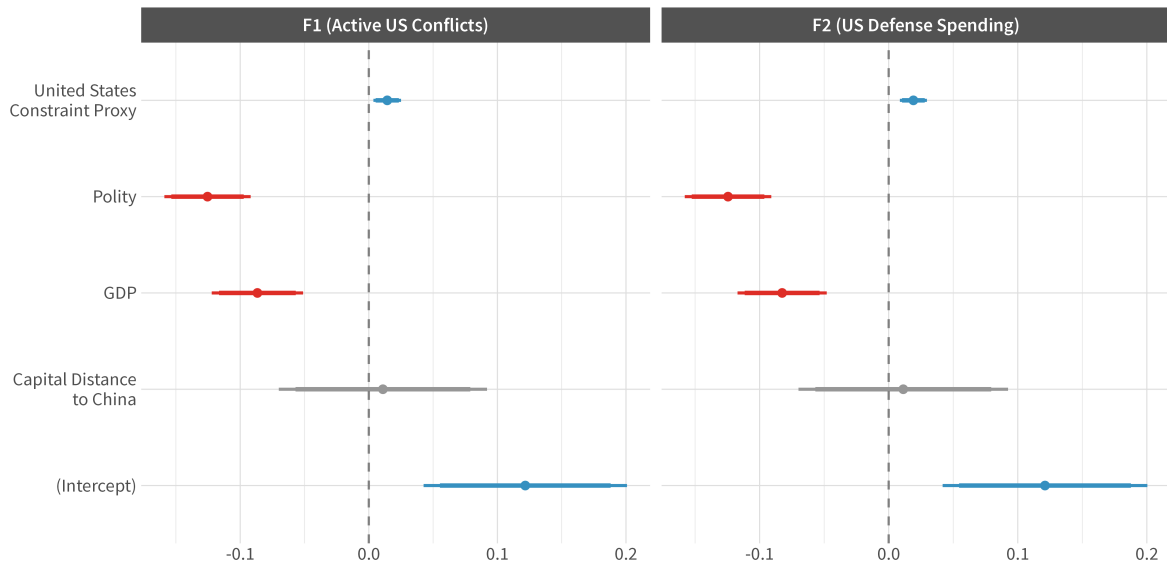


Figure A6: Parameter estimates from hierarchical model on diplomatic similarity with random country effects. Each column shows the results with a different distraction measure that is labeled in the facet on the top of the plots. Points represent average value of parameters, thicker line represents the 90% confidence interval, and thinner the 95%.

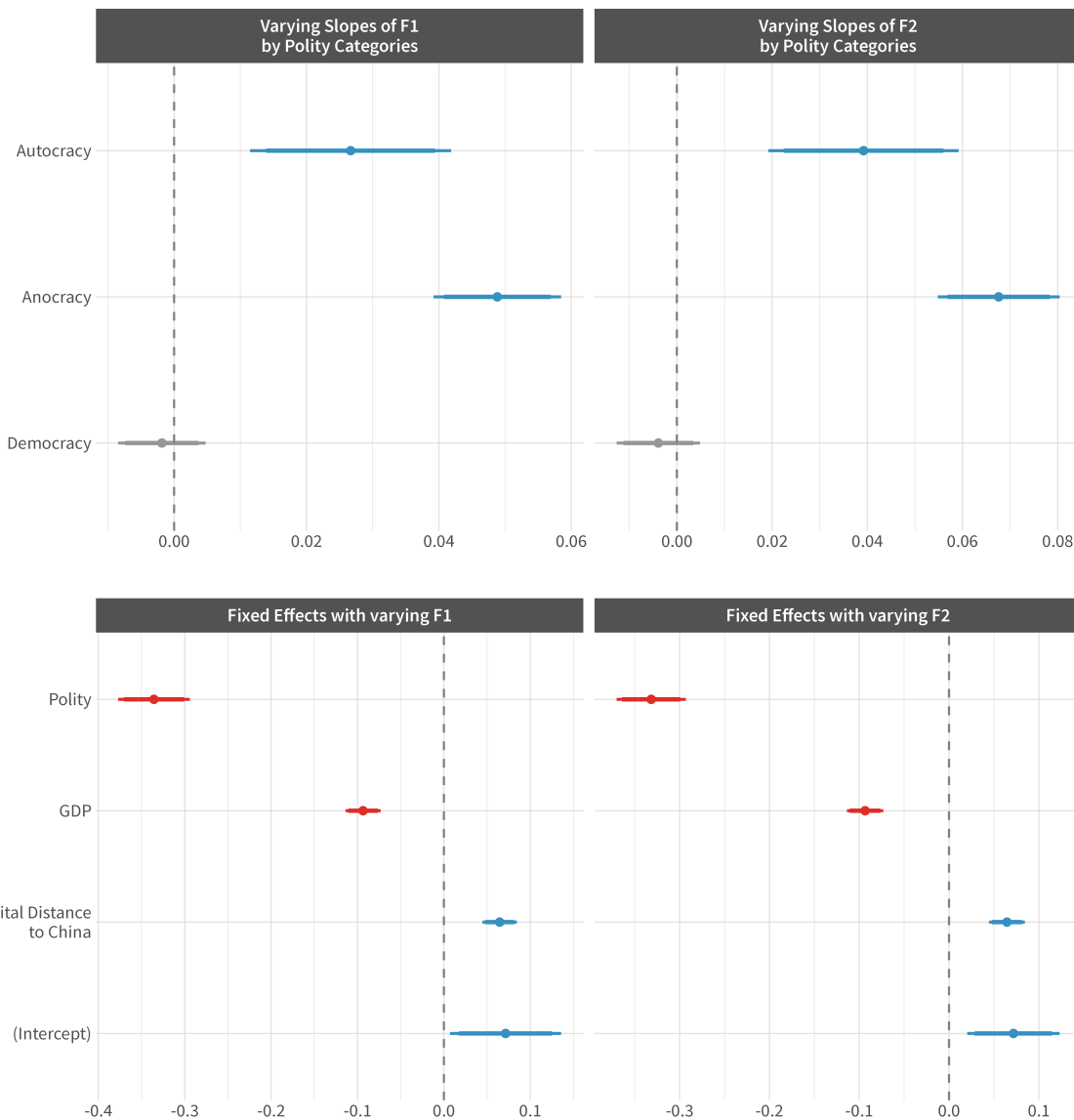


Figure A7: Parameter estimates from hierarchical model on diplomatic similarity with varying effects of the distraction measures by polity categories. Top panel shows how the distraction measures vary by polity categories and bottom the fixed effects, each column again represents the results of one model. Points represent average value of parameters, thicker line represents the 90% confidence interval, and thinner the 95%.

A.4. Country Fixed Effects Robustness Check

In addition to the model results presented in Figure 6, we estimate another with country fixed effects to account for any time-invariant heterogeneity (e.g., geography, shared history, cultural ties). This ensures that our main findings are not driven by stable country-level features that might correlate with alignment decisions. Figure A8 shows the coefficient estimates from this fixed-effects version.

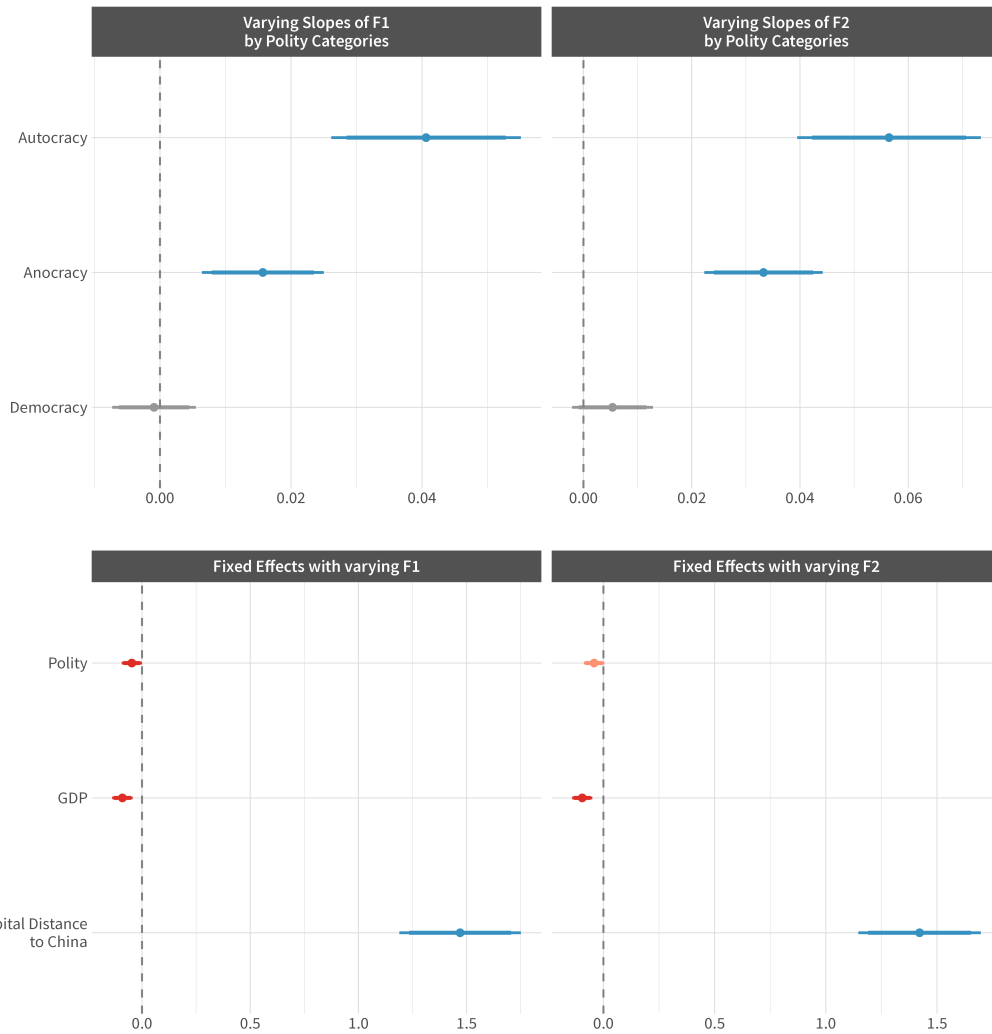


Figure A8: Parameter estimates from hierarchical models of diplomatic alignment with varying effects of the distraction measures by regime type *and* country fixed effects. The top panel shows the coefficients for our distraction measures interacted with polity categories, and the bottom panel shows the fixed effects. Points represent posterior means; thicker lines indicate 90% credible intervals, and thinner lines indicate 95%.

Across these fixed-effects models, we continue to observe that:

1. *Higher U.S. Distraction* —→ *More Alignment with China (Autocracies/Anocracies)*. States with less democratic institutions remain most responsive to U.S. constraint.
2. *Democracies Resist Closer Alignment with China*. Our results for fully democratic regimes remain consistent with the baseline, showing a weaker or even negative relationship between U.S. distraction and alignment with China.

These core dynamics align closely with our primary analyses, suggesting that our conclusions are robust to the inclusion of country-specific intercepts.

A.5. Simulation Study for Latent Factor Measurement

In this appendix, we conduct a small-scale simulation to experiment with our use of the LFM when only *aggregated* co-voting rates (rather than individual-level vote choices) are observed. This is meant to help understand how individual votes might plausible arise from latent positions and whether the LFM can recover those positions from the aggregated data.

In many legislative and judicial roll call models (e.g. IRT, NOMINATE, or Martin–Quinn), there is a well-defined mapping from an actor’s latent “ideal point” to their vote choice on each item. In our setting, however, we only provide as an input to the LFM the fraction of times each pair of states cast the same vote in the United Nations. This simulation shows a scenario in which

1. Each state *and* each resolution is placed in a low-dimensional latent space.
2. The probability that a state votes “Yes” on a given resolution depends on the dot product of their respective latent coordinates.
3. We aggregate these yes/no outcomes across resolutions to form a matrix of co-voting rates between every pair of states, akin to our main data setup.
4. Finally, we fit the LFM to the aggregated data and assess whether the recovered latent positions align (up to rotation/reflection) with the known true coordinates.

If we find that the estimated latent positions align closely with the known “true” coordinates, it indicates that this procedure can effectively uncover higher-order structure in the data—despite relying only on a *similarity matrix* summarizing the fraction of co-votes between pairs of actors.

A.5.1. Data-Generating Process for Votes

We simulate $n = 50$ states and $m = 300$ resolutions (“votes”), each situated in a 2D latent space:

1. *True State Positions* (\mathbf{U}_{true}): We draw a 50×2 matrix from a normal distribution. Each row represents a state’s “foreign-policy orientation” in this 2D space.
2. *Resolution Positions*: Similarly, we assign each of the 300 resolutions a 2D coordinate. Intuitively, a resolution’s location might capture its ideological or policy dimension.
3. *Vote Generation*: For state i and resolution m , the probability of a “Yes” vote is

$$\Pr(\text{Yes}_{i,m}) = \Phi(\beta_0 + \langle \mathbf{U}_{\text{true},i}, \mathbf{IssuePositions}_m \rangle),$$

where $\Phi(\cdot)$ is the cumulative distribution function of the normal distribution, β_0 is an intercept, and $\langle \cdot \rangle$ denotes the dot product. We then draw a Bernoulli random variable to determine whether state i votes “Yes” or “No.”

After simulating all 300 resolutions, we construct a 50×50 co-voting matrix \mathbf{Y} where

$$Y_{ij} = \text{fraction of votes on which } i \text{ and } j \text{ both vote "Yes" or both vote "No".}$$

We set $Y_{ii} = \text{NA}$.

We next fit the LFM to our simulated co-voting matrix using a normal model for continuous outcomes in $[0, 1]$. Because the co-voting data are symmetric, we set the model to estimate a single latent position per actor. The result is a set of estimated coordinates for each state, which we compare to the true latent positions via a Procrustes transform (aligning rotations and reflections). This yields correlation measures indicating how well the recovered latent space matches the data-generating structure.

A.5.2. Assessing Recovery of the True Positions

Since any latent factor model is invariant to rotation, reflection, or translation, we apply a Procrustes transform to align the estimated positions, $\hat{\mathbf{U}}$, with the known true positions, \mathbf{U}_{true} . We then compute correlations along each dimension:

$$\rho_{\text{dim1}} = \text{corr}(\mathbf{U}_{\text{true}}[:, 1], \hat{\mathbf{U}}_{\text{aligned}}[:, 1]), \quad \rho_{\text{dim2}} = \text{corr}(\mathbf{U}_{\text{true}}[:, 2], \hat{\mathbf{U}}_{\text{aligned}}[:, 2]),$$

and an overall correlation by flattening the matrices into vectors. We find strong absolute correlations (e.g., $|\rho| \geq 0.85$), indicating that the LFM successfully recovers the underlying structure from the aggregated co-voting matrix.

This simulation thus demonstrates a coherent “first-principles” path from *individual-level vote choices* to an aggregated *similarity matrix*, and then back to *latent positions*. Even though the LFM does *not* observe individual votes, it accurately recovers the 2D structure that generated those votes once we transform them into a co-voting measure. This outcome strengthens our empirical strategy, suggesting that a similar process may hold in real-world UN voting: modeling \mathbf{Y} via an LFM can capture higher-order positioning in joint decision-making contexts.

References

- Frieden, Jeffry A., David A. Lake, Michael Nicholson and Aditya Ranganath. 2017. "Economic Crisis and Political Change in the United States, 1900 to the Present." *Unpublished manuscript, University of California, San Diego* .
- Kane, Tim. 2016. "The decline of American engagement: Patterns in US troop deployments." *Economics working paper* 16101.
- Trading Economics. 2021. "Trading Economics Data."
URL: <https://tradingeconomics.com/>
- US Department of Defense. 2020. "National Defense Budget Estimates for Fiscal Year 2021." *Office of the Under Secretary of Defense (Comptroller)* .
URL: https://comptroller.defense.gov/Portals/45/Documents/defbudget/fy2021/FY21_Green_Book.pdf
- World Bank. 2021. "World Bank Open Data.".
URL: <https://data.worldbank.org/>